



Fuzzy logic, neural-fuzzy network and honey bees algorithm to develop the swarm motion of aerial robots

Iman Shafieenejad¹ · Elham Dehghan Rouzi² · Jamshid Sardari³ · Mohammad Siami Araghi³ · Amirhosein Esmaeili⁴ · Shervin Zahedi¹

Received: 23 April 2020 / Accepted: 31 May 2021

© The Author(s), under exclusive licence to Springer-Verlag GmbH Germany, part of Springer Nature 2021

Abstract

In this study, a novel nature-inspired autonomous motion was investigated using the honey-bee algorithm for aerial robots. The main idea belonged to a novel analogy between optimal honey bees and aerial robots' motion in proposing autonomous guidance. Three-dimensional simulations for aerial robots were considered to show the efficient performance of autonomous guidance. A new equation system was also developed based on the yaw angle control to simplify dynamic flight calculations. Moreover, different uncertainties such as lateral wind current and navigation' noise were considered and checked precisely using a neural-fuzzy network to enhance autonomous guidance reliability. Accordingly, aerial robots' autonomous motions were developed by fuzzy logic to overcome low-quality data linkages between aerial robots. The results of this study illustrated that the integrated nature-inspired guidance by fuzzy logic had a lower total passing and the final time of 24.64% and 21.87% for aerial robots, respectively.

1 Introduction

Autonomous aerial robots with closed-loop guidance are of paramount importance for civil missions. Further research and ideas are required for conventional guidance methods to develop the next generations of aerial robots. The usual open-loop guidance methods are underpinned by the ground station; therefore, the reduction of ground station commands by novel intelligent methods is essential for the next aerial robots' development. Moreover, many studies have examined closed-loop guidance using artificial intelligence methods to remove uncertainties (Al-Rabayah and Malaney 2012; Babaei et al. 2011; Bernsen and Manivannan 2012; Bitam et al. 2013; Chen et al. 2016, 2017; Dadkhah and Mettler 2012; Eng et al. 2010). The problem statement, the main

contributions and the motivation of this paper are as follow. The main problem of this paper is belonged to propose a novel nature-inspired autonomous motion of arial robots with artificial intelligence. The idea of this paper represented a novel analogy between optimal honey bees and aerial robots' motion in proposing autonomous guidance. Moreover, to explain the motivation of this paper, new equation system was also developed based on the yaw angle control to simplify dynamic flight calculations. Furthermore, different uncertainties such as lateral wind current and navigation' noise were considered using a neural-fuzzy by training a network to develop autonomous guidance reliability. Also, aerial robots' autonomous motions were enhanced by fuzzy logic to overcome low-quality data linkages between aerial robots as a closed-loop guidance method.

Different guidance methods, especially closed-loop and autonomous algorithms, are valuable for aerial robots to enhance the precision of online path planning. Hence, many studies have focused on novel methods such as machine learning and the Internet of Things (IoT). Novel methods address problems such as low-quality information linkages and low-accuracy targets looking for autonomous aerial robots; therefore, their contributions have been demonstrated. Mavrovouniotis et al. (2017) studied the changes in the dynamics of swarm intelligence algorithms to increase their performance (Fallah-Zazuli et al. 2019). Mettler and

✉ Iman Shafieenejad
shafiee_iman@yahoo.com

¹ A & S Research Institute, Ministry of Science Research and Technology, Tehran, Iran

² Faculty of Electrical and Computer Engineering Islamic Azad University, Tehran North Branch, Tehran, Iran

³ Department of Aerospace Engineering, Science and Research Branch, Islamic Azad University, Tehran, Iran

⁴ School of Automotive Engineering, Iran University of Science and Technology, Tehran, Iran

Dadkhah investigated autonomous guidance using optimization methods.

Furthermore, the primary system was integrated based on the cost function and approximation using the optimal path planning (Goerzen et al. 2010). Rajasekhar et al. (2017) represented the engineering applications of swarm intelligence optimization algorithms. In Hoffer et al. (2014), some engineering applications of the honey-bee optimization method are illustrated. In Huang et al. (2016), Laomettachit et al. (2015) performed the bifurcation analysis and stochastic simulations in honey-bee swarms using adaptive decision-making. Moreover, Luo et al. (2019) represented the swarm intelligence algorithm as MSAAs using a new elite position-based method (Lange et al. 2009). Zedadra et al. (2018) discussed decentralized systems, including honey-bee algorithms, in Laomettachit et al. (2015). Some advantages such as self-organization and potentials to overcome the complex problems of incomplete and limited information in the computation were also investigated. Moreover, the advantages of the IoT application were examined by Zedadra et al. (2018) to develop the new guidance methods. In Liu et al. (2016), Zhou studied autonomous three-dimensional guidance for aerial robots with different cost functions.

In Luo et al. (2019), a k-degree smoothing method for trajectory design was proposed considering a complex environment for multiple sources. Both artificial intelligence and particle swarm optimization were considered in combination with the adaptive algorithm for optimal trajectory in Ma et al. (2006). In Mavrovouniotis et al. (2017), an encoding approach was proposed using the two-part wolf pack search algorithm for multiple autonomous aerial robots to avoid complex environments and check uncertainties. Moreover, genetic, birds swarm, random search, and firefly algorithms were included under the same conditions. The findings in Mettler et al. (2010) illustrated that most autonomous guidance methods had an actual performance for aerial robots' real dynamic model, thereby enhancing the system's reliability. Furthermore, three-dimensional online guidance was proposed for the trajectory optimization of aerial robots (Moayedi and Hayati 2018a). Lange et al. proposed a guidance algorithm for aerial robots by estimating the relative altitude and position (Moayedi and Hayati 2018b). Similarly, many studies have focused on relevant topics such as system identification approaches for low-cost aerial robots (Moayedi et al. 2020), trajectory planning with and without environment differential constraints, aerial robots' autonomous guidance under uncertain conditions, helicopter navigation and control techniques, and state estimation for aerial robots (Moayedi and Rezaei 2019).

In this study, novel guidance was presented based on the analogy between optimal honey-bee motion and aerial robots' guidance. The new analogy was described, and three-dimensional simulations were established. Moreover, the

neural-fuzzy network was trained to avoid different uncertainties such as lateral wind current and navigation system' noise. Moreover, fuzzy logic was studied to overcome low-quality data linkages between aerial robots. The results showed the potentials of the proposed method for autonomous aerial robots to have robust closed-loop guidance.

2 Literature review

One of the major studies in this field belongs to Moayedi et al. (2019), who described the primary sources of uncertainty arising in aerial robots' guidance and the relevant practical techniques. They compared the contributions of robotics and artificial intelligence with those of the dynamic systems and controls. These fields' contributions were highlighted, providing a roadmap to tackle with the aerial robot guidance problem using the intelligence method. Hence, a novel method for autonomous aerial robots should be proposed using the artificial bee algorithm.

Moreover, the neural-fuzzy network was considered to reduce lateral wind current and navigation noise. The other studies have not addressed these two types of uncertainties simultaneously. In Mosallanezhad and Moayedi (2017), several non-linear machine learning models such as feedforward neural network, radial basis neural network, general regression neural network, support vector machine, tree regression fitting model, and adaptive neuro-fuzzy inference system were investigated and compared. Then, the predicted findings of the models were compared with those of the finite element data. The findings showed a good agreement in terms of reliability for the feedforward neural network. The other applications of machine learning models were presented in Nguyen et al. (2019), in which an artificial neural network investigated an engineering problem, and the results were highly accurate. The proposed approach had high agreement with a lower mean absolute error, compared to the other methods. Moreover, the presented models' accuracy was investigated using the value of root-mean-square error and regression plots in Paw and Balas (2011).

The development of a spatially explicit deep learning neural network model was studied to predict landslide susceptibility in Rajasekhar et al. (2017). According to the findings, the deep learning neural network model provided accurate results. Furthermore, the efficiency of the model was compared to that of the quadratic discriminant analysis, Fisher's linear discriminant analysis, and multi-layer perceptron neural network. One of the main advantages of machine learning models is their combination with optimization methods. Hence, the artificial neural network's capability was synthesized with artificial bee colony, and the particle swarm optimization algorithms were investigated in Samani et al. (2015). The findings demonstrated that training the artificial

neural network with artificial bee colony and particle swarm optimization algorithms enhanced the network’s reliability. The combination of the artificial neural network with the particle swarm optimization algorithm provided the most accurate results. In Torres et al. (2016), various evolutionary artificial intelligence and machine learning models were optimized using the artificial neural network, particle swarm algorithm, differential evolution algorithm, adaptive neuro-fuzzy inference system, general regression neural network, and feedforward neural network. In this regard, a combination of an imperialist competitive algorithm and an artificial neural network was proposed in Zedadra et al. (2018), and the artificial neural network was improved by being optimized with an imperialist competitive algorithm.

Furthermore, the multi-layer perceptron neural network was optimized with the artificial bee colony and particle swarm algorithms. The results revealed that the use of the artificial bee colony and particle swarm optimization algorithms improved the multi-layer perceptron neural network’s efficiency (Zhou et al. 2020). In Zhou et al. (2019), the efficiency of the proposed neural model of the artificial neural network optimized with particle swarm in estimating the safety factor, compared to other machine learning methods, was investigated. Moreover, the neuro particle-based optimization of the artificial neural network was studied, and the results were compared with the conventional artificial neural network and adaptive neuro-fuzzy inference system training solutions. According to the findings, the artificial neural network optimized by particle swarm optimization algorithm performed slightly better than the conventional artificial neural network algorithms.

3 Novel guidance for autonomous aerial robots

Food sources (flower nectar) and bees are two main parts of honey-bee swarm motion. In this study, bees and food sources were considered as aerial robots and artificial targets, respectively. The main target was considered as the best nectar. An initial population of the algorithm for different artificial targets was selected randomly. Search space (main domain) is defined by the minimum and maximum values of motion bounds, where the main target is placed. Accordingly, the three bounds are considered in Eq. (1).

$$\bar{X} = \{X_{\min}, X_{\max}\}, \bar{Y} = \{Y_{\min}, Y_{\max}\}, \bar{Z} = \{Z_{\min}, Z_{\max}\} \quad (1)$$

A place in the above cubic domain is taken in $[\bar{X}, \bar{Y}, \bar{Z}]$. Like bees in the Artificial Bee Colony algorithm (ABC), the aerial robots are of three types. Worker, onlooker, and scout bees are named A, B, and C, respectively. Aerial robots, as A-type, have initial random roles. In this algorithm, A-type

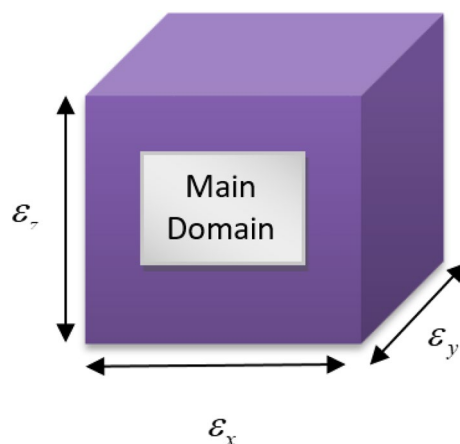


Fig. 1 Three-dimensional bounds/cubic domain

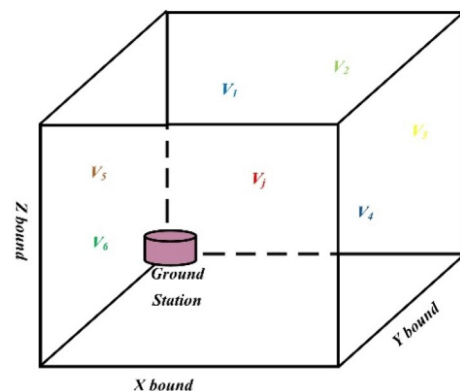


Fig. 2 Random positions of aerial robots in cubic domain

aerial robots’ positions are randomly distributed in the main domain. These are called zero positions (X0, Y0, Z0). Later, aerial robots move from (X0, Y0, Z0) to the next positions (Xi*, Yi*, Zi*). The index (i) represents the number of aerial robots. Moreover, the bounds of search space are determined as $\epsilon_x, \epsilon_y, \epsilon_z$. Furthermore, X^*, Y^*, Z^* are derived based on Eqs. (2–5) (Figs. 1 and 2). In Fig. 2, V_N (N is the number of aerial robots) represents aerial robots’ random positions with random initial velocities. R

$$\left| \begin{matrix} \bar{X} \\ \bar{X} \end{matrix} \right|_{\max} - \left| \begin{matrix} \bar{X} \\ \bar{X} \end{matrix} \right|_{\min} = \bar{\epsilon} \quad (2)$$

$$\bar{\epsilon} = [\epsilon_x \ \epsilon_y \ \epsilon_z] \quad (3)$$

$$\bar{X} = [X \ Y \ Z] \quad (4)$$

$$\bar{X}_i^* = \left\{ \frac{|\bar{X}_{\max}| + |\bar{X}_{\min}|}{2} \right\} + \left\{ |rand| \leq \left| \bar{\epsilon} / 2 \right| \right\} \quad (5)$$

In the above equations, $|rand|$ denotes a random number smaller than $\epsilon_k/2(k = x, y, z)$, and X_i^*, Y_i^*, Z_i^* represent the next position of the i th aerial robot in the cubic domain. According to the ABC algorithm, the second positions of aerial robots are achieved randomly. A flowchart of the proposed nature-inspired guidance is illustrated in Fig. 3.

A-type aerial robots search for artificial targets and memorize their positions. Then the new artificial targets are updated and shared with the B-type aerial robots. B-type aerial robots search for the closest artificial targets. The third role of aerial robots belongs to the C-type when an artificial target is not improved after a limited number of searches. Accordingly, the C-type aerial robots contribute to the achievement of better targets and replace them with the last artificial targets. Hence, the C-type aerial robots improve the algorithm to find the best artificial target in the defined domain. For each artificial target, A-type bees generate new motions to search the next artificial targets and their neighborhood using the following equation:

$${}^m\bar{\zeta}_n^j = {}^m\zeta_n^j + \sigma_n^j \left({}^m\zeta_n^j - {}^m\zeta_k^j \right) \quad (6)$$

where $m \in \{x, y, z\}$, $j \in \{1, 2, 3, \dots, N\}$, and N is the number of aerial robots. The index k denotes the random targets that may help updating artificial targets, n is the iteration in the mentioned algorithm, and $k = n - 1$. Moreover, σ_n^j is a random value in the range of $[-1, 1]$, which causes random motions.

One of the most remarkable features of bees is nutation dancing. When A-type aerial robots return to the hive, they transform the information of artificial targets to the B-type aerial robots by their nutation signals. A target selected by the B-type aerial robots is denoted by P_n .

$$P_n = \frac{fit_n}{\sum_{m=1}^N fit_m} \quad (7)$$

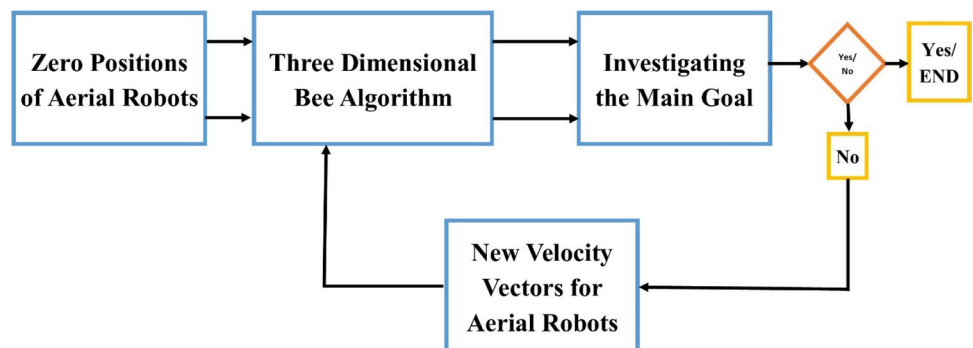
The qualities of artificial targets are demonstrated by fit_n . The aerial robots transfer the position information in this way; hence, aerial robots with more fuel will remain. Finally, some artificial targets cannot be searched by A- and B-types. Consequently, C-type aerial robots are sent to search the main domain. C-type aerial robots help the algorithm find unsearched artificial targets. In other words, this algorithm can overcome the difficulties in finding the global/main target. This is one of the advantages of this algorithm, which can be used as novel guidance for aerial robots.

The mentioned guidance can take place in eight steps: (1) the first step refers to the initial motion of aerial robots and is completely random in the defined domain, (2) distances from artificial targets are evaluated, (3) stopping criterion is likely to occur, or a new distribution is formed. In this step, the aerial robots' swarm motion is formed while the stopping criterion (finding the primary target) is met, (4) neighborhood is searched to find the minimum distance from artificial targets, (5) the employment of aerial robots for selected artificial targets is considered, and distances are re-evaluated, (6) the main target is selected based on the distance values for aerial robots, (7) to increase the potentials of the mentioned algorithm, the remaining aerial robots are assigned to search randomly, while evaluating their distances by other aerial robots, and (8) finally, the algorithm is finished by the while-loop considered in the third step.

4 Decreasing uncertainties by neural-fuzzy network

The present study has two main novelties. The first one is to consider the artificial bee algorithm for path planning and to regard an analogy between bee motion and aircraft. Since the bee motion algorithm is optimal naturally, the aerial robot swarm's motion is considered optimal. The second novelty

Fig. 3 Flowchart of novel proposed guidance based on the honey bee algorithm



is to decrease uncertainties concerning lateral wind current and navigation system' noise by the neural-fuzzy network.

A neural-fuzzy network is a powerful method for machine learning, decision-making, and response predicting in a complex system to cover uncertainties and increase the dynamic system's reliability (Al-Rabayah and Malaney 2012; Babaei et al. 2011). The state variable \vec{u} and time t influence the control part of a dynamic system \vec{x} , $\vec{u} = \vec{u}(\vec{x}, t)$. Dynamic systems with no robust controllers against noise are weak in operation and less reliable. Any disturbances in the initial conditions and noise along the path can make the system deviate from the pre-designed trajectory. In a system with high reliability, if noise is added to the dynamic system, it can reduce noise and return to the main path, so $\vec{u} = \vec{u}(\vec{x})$.

To implement the neural-fuzzy intelligent system, several flight scenarios are selected from the simulation of the last section. Accordingly, three flight scenarios are selected so that the neural-fuzzy network accomplishes the dynamic system training by artificial intelligence.

The simulation' results from the autonomous bee algorithm in the previous section are given to the neural-fuzzy network for training. First, the validity of the trained system should be examined. Then, one of the results of the trained neural-fuzzy network is examined for an already-simulated scenario.

Figure 4 shows the validity of the training procedure. As presented in the figure, 390 training data are demonstrated by o, and the output of the neural-fuzzy network is indicated by *. Hence, when o and * are matched, the training procedure is matched precisely as well.

The dynamic system is trained accurately with an error rate below 0.00020963. Moreover, the number of iterations for training is expressed by epoch number as 10. Once the neural-fuzzy network training is assured, the results will be encrypted as software in the artificial bee algorithm's dynamic system. In this method, the membership functions are tuned optimally based on the artificial neural network's training input data. Regarding uncertainty in the initial conditions, the control variable corresponding to the state vector is generated from the neural-fuzzy network output as the

yaw control angle. The output of the neural-fuzzy network is the trained yaw control angle $\varphi(t)$, and the horizontal line (number of data) is the number of data considered for three scenarios presented in Table 1.

Furthermore, the generated network by the neural network is illustrated in Fig. 5. As shown in the figure, four inputs with three separate membership functions are considered to construct the neural-fuzzy network. Moreover, all inputs are correlated and engaged with an output. Furthermore, the backpropagating method is used in the fuzzy inference system for training data.

Accordingly, closed-loop guidance is achieved for the mentioned aerial vehicles. The training scenarios for the neural-fuzzy network are described in Table 1.

5 Uncertainties

In this work, two types of uncertainties are considered to check the mentioned intelligent guidance's reliability. The first is the environment effect on the lateral wind current, and the second is the noise exerted on the dynamic navigation system by noisy state variables. For uncertainties in lateral wind current, three modeled lateral wind currents are considered based on

Table 1 Three scenarios trained by neural-fuzzy network

Scenario	Initial condition	Final condition
First scenario	$x_0 = 100$ (m)	$x_f = 0$ (m)
	$y_0 = 195$ (m)	$y_f = 0$ (m)
	$z_0 = 65$ (m)	$z_f = 0$ (m)
Second scenario	$x_0 = 90$ (m)	$x_f = 0$ (m)
	$y_0 = 205$ (m)	$y_f = 0$ (m)
	$z_0 = 75$ (m)	$z_f = 0$ (m)
Third scenario	$x_0 = 95$ (m)	$x_f = 0$ (m)
	$y_0 = 200$ (m)	$y_f = 0$ (m)
	$z_0 = 85$ (m)	$z_f = 0$ (m)

Fig. 4 Validation of the neural-fuzzy network

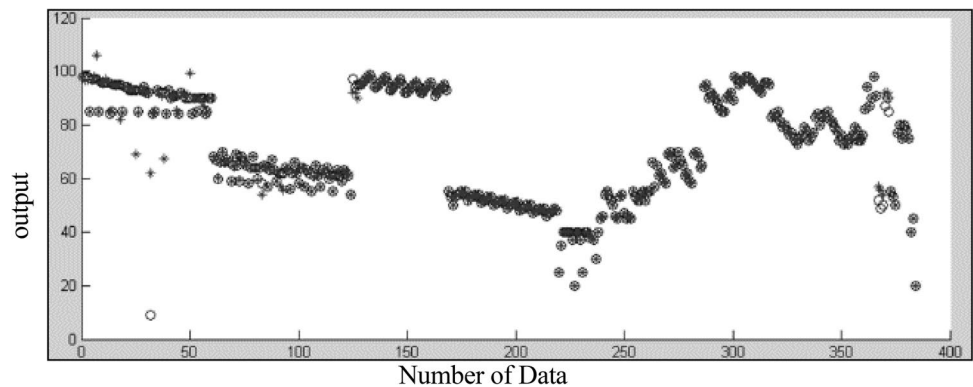
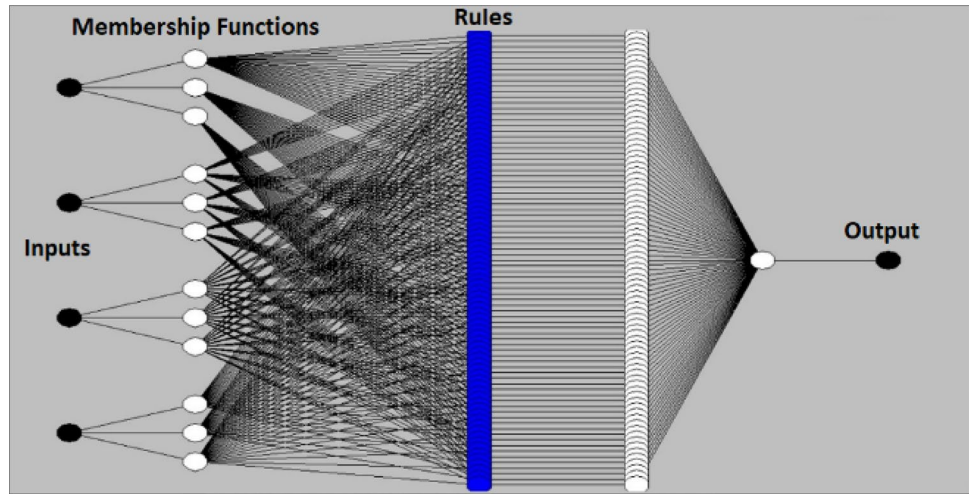


Fig. 5 Neural-fuzzy network



Eqs. (8)–(10) for three dimensions of x, y, z . In these equations, the lateral wind’s relative speed is $V=20$ (m/s) in the height of $h=50$ (m). Hence, the lateral wind is formulated as follows:

$$v = -(V/h)x \tag{8}$$

$$u = -(V/h)y \tag{9}$$

$$w = -(V/h)z \tag{10}$$

Moreover, the random numbers are added to the model for precise modeling of lateral wind current to show the neural-fuzzy network’s reliability.

$$v = u = w = -\left(\frac{V}{h}\right)(1 + \sigma) \tag{11}$$

$\sigma \in [0 \ 0.1]$; *Random Number*

Figure 6 demonstrates the second type of uncertainties exerted on the navigation system.

$$\vec{x}_{noisy} = \vec{x} + \delta\vec{x} \tag{12}$$

In Eq. (12), the noise vector $\delta\vec{x}$ is an action on the dynamic system or state variables concerning the navigation system’s fault. The equations below demonstrate noise in the state variables x, y, z .

$$\delta x(t) = 0.5 \sin(10\theta(t))x(t) \tag{13}$$

$$\delta y(t) = 0.5 \sin(10\theta(t))y(t) \tag{14}$$

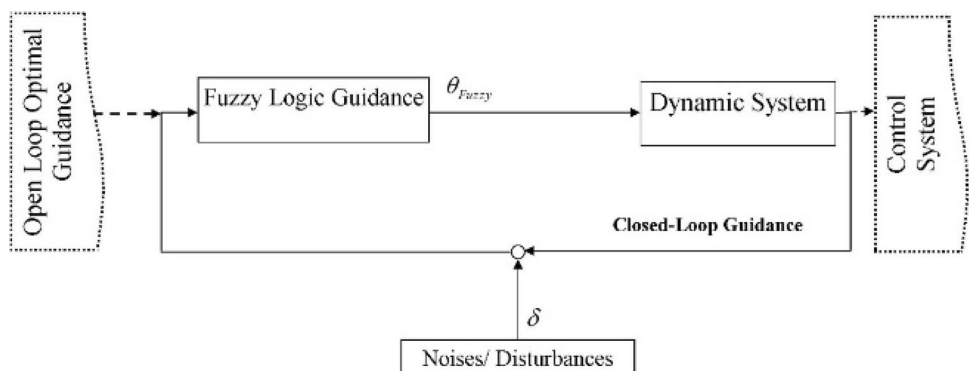
$$\delta z(t) = 0.5 \sin(10\theta(t))z(t) \tag{15}$$

6 Kinematic equations

The motion equations for the mentioned aerial robots are modeled as the point mass equations for achieving aerial robot guidance.

$$\frac{dx}{dt} = V \cos(\varphi) \cos(\psi) + u \tag{16}$$

Fig. 6 Applied noise to the dynamic system



$$\frac{dy}{dt} = V \cos(\varphi) \sin(\psi) + v \tag{17}$$

$$\frac{dz}{dt} = V \sin(\varphi) + w \tag{18}$$

Figure 7 illustrates the schematics of aerial robots' coordinates. In Eqs. (16–17), lateral wind speeds are considered as u, v, w . Further, there are two control angles of pitch and yaw as $\psi(t), \varphi(t)$ in the mentioned differential equations, respectively. In this paper, the first derivatives of the two mentioned angles, $\frac{d\varphi}{dt}, \frac{d\psi}{dt}$, are obtained from the simulations of the bee algorithm. Moreover, a mathematical relationship is established between the two angles. The relationship between these two control angles are expressed as:

$$\frac{d\varphi}{d\psi} = \frac{d\varphi/dt}{d\psi/dt} \tag{19}$$

In this section, the output of the neural-fuzzy network is considered $\varphi(t)$. The new differential equations are considered and integrated, $d\varphi$ instead of dt .

$$\frac{dx}{d\varphi} = \frac{1}{(d\varphi/dt)}(V \cos(\varphi) \cos(\psi) + u) \tag{20}$$

$$\frac{dy}{d\varphi} = \frac{1}{(d\varphi/dt)}(V \cos(\varphi) \sin(\psi) + v) \tag{21}$$

$$\frac{dz}{d\varphi} = \frac{1}{(d\varphi/dt)}(V \sin(\varphi) + w) \tag{22}$$

The proposed neural-fuzzy network can deliver the aerial robots using the above dynamic system with high reliability, while considering uncertainties from the initial point to the endpoint as an online process.

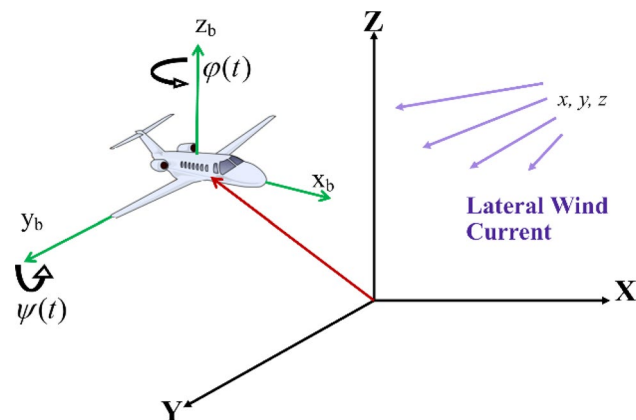


Fig. 7 Schematics of aerial robots coordinate and lateral wind current

The following figures show the results. In each of Figs. 8, 9, 10, 11, 12 and 13, three series of data are presented. Graphs for “Open-Loop without Noise” show one of the aerial robots’ flight simulations to reach the target. Graphs for “Closed-Loop with Noise” show the dynamic systems’ exerted noise, where the neural-fuzzy network can decrease the noise precisely. Therefore, graphs for “Closed-Loop with Noise” are completely consistent with graphs for “Open-Loop without Noise”. On the other hand, graphs for “Open-Loop with Noise” show the dynamic system’s exerted noise without considering the neural-fuzzy network. Evidently, the aerial robot is out of its path and has no resistance to the noise.

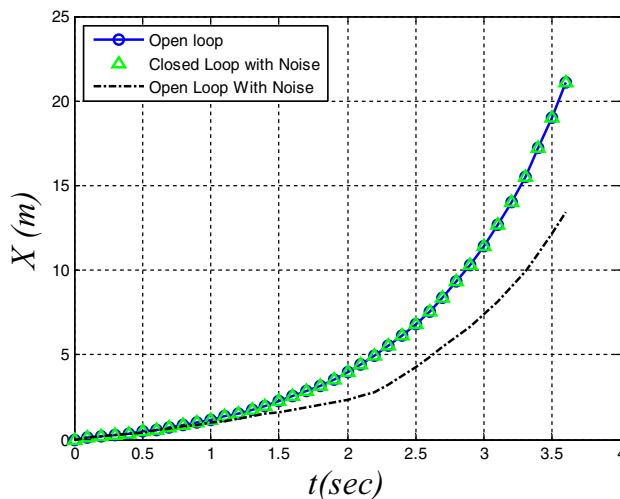


Fig. 8 Time history of $x(t)$ regarding damping uncertainties

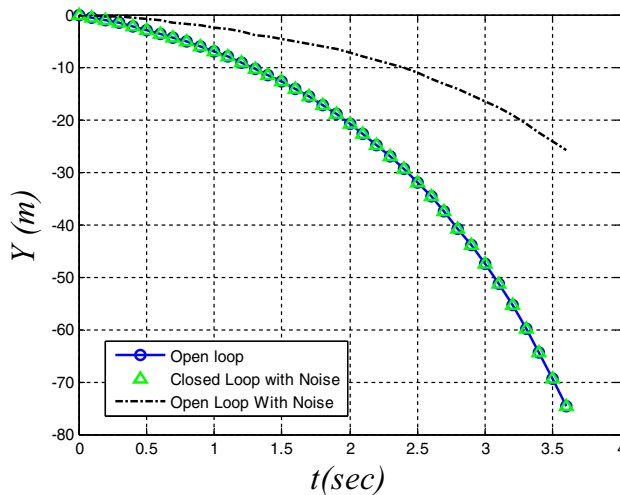


Fig. 9 Time history of $y(t)$ regarding damping uncertainties

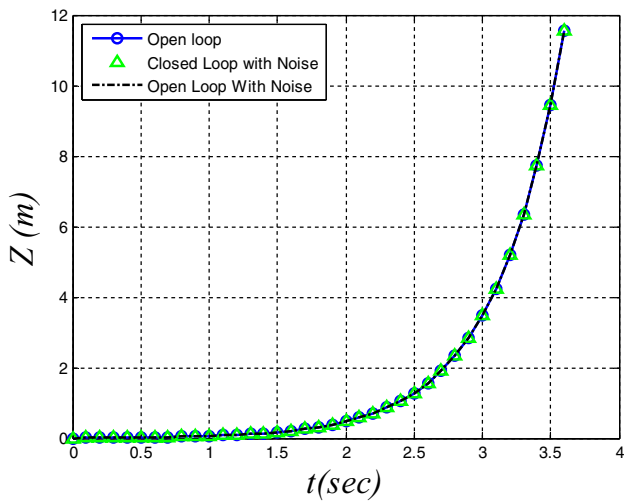


Fig. 10 Time history of $z(t)$ regarding damping uncertainties

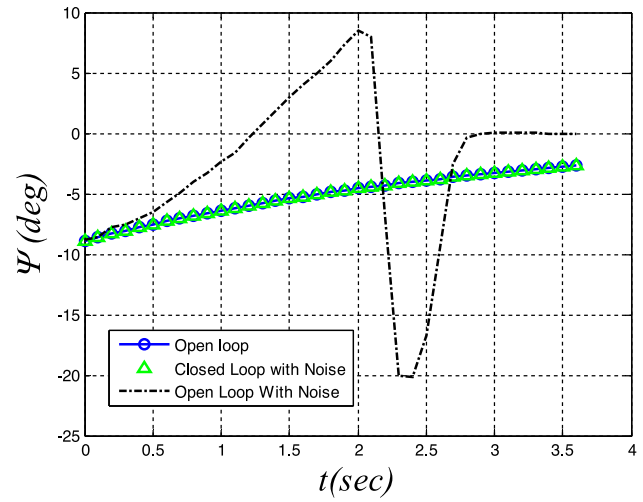


Fig. 12 Time history of $\psi(t)$ regarding damping uncertainties

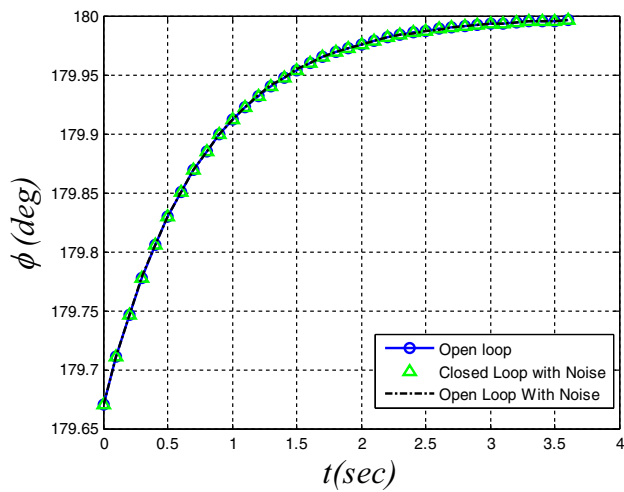


Fig. 11 Time history of $\varphi(t)$ regarding damping uncertainties

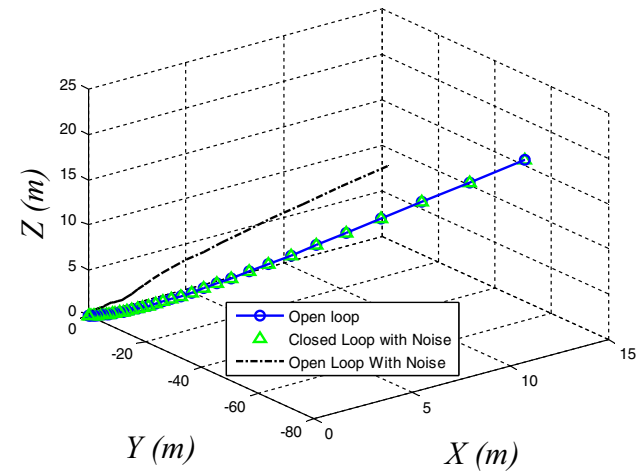


Fig. 13 Three-dimensional trajectory regarding damping uncertainties

Figure 9 shows the divergence open loop with noise. Also, it is obvious aerial robots by open loop with noise diverges.

Figures 8, 9 and 10 demonstrate one of the aerial robots' motion in three directions of x , y , z . The divergence of aerial robots when noise is exerted on the dynamic system without considering the neural-fuzzy network is shown in Figs. 8 and 9. Therefore, intelligent guidance by the neural-fuzzy network offers a robust response to enhance the reliability of aerial robots' motions against the lateral wind current.

Figure 11, demonstrates the yaw angle regarding open loop, open loop and closed loop with noise. Results show the yaw angles of aerial robots have the robust responses against noise. Hence, the yaw angle is independent of noise regarding Eqs. (20–22).

The pitch angle has divergency due to the exerted noise in the graph “Open-Loop with Noise”, as illustrated in Fig. 12. Hence, closed-loop guidance by the neural-fuzzy network provides precise results to reduce the noise effect on the dynamic system. The three-dimensional motion of one of the aerial robots is shown in Fig. 13.

Further, another test to determine the accuracy of the training process by the neural-fuzzy network was applied. Hence, the trained artificial system robustness was investigated to decrease the noise inserted on the control variable. Here, noise is considered as follows:

$$\varphi_{noisy}(t) = \varphi(t) + \delta\varphi(t) \tag{23}$$

The applied noise $\delta\varphi$ to the dynamic system is formulated by Eq. (24).

$$\delta\varphi(t) = 0.25 \sin(10\varphi(t))\varphi(t) \tag{24}$$

In Figs. 14, 15 and 16, blue triangle graphs illustrate the open-loop guidance without considering noise; black lines demonstrate the noise by considering the neural-fuzzy network; and red dotted lines show the results without considering the neural-fuzzy network.

Figure 14 demonstrates the x direction with and without noise. Red dotted line shows divergence of an aerial robot without considering neural-fuzzy network. Hence, the aerial robot regarding considering neural-fuzzy network has precise x direction.

As observed in Fig. 14, the neural-fuzzy network can decrease the noise exerted on the yaw control angle. According to Figs. 15 and 16, the exerted noise on the yaw control angle does not affect the y and z directions of motion. The trained neural-fuzzy network can overcome the system noise, and the reliability of the designed intelligent system increases, as shown in Figs. 14, 15 and 16. Hence, intelligent guidance can follow the main path.

7 Enhancing position of aerial robots by fuzzy logic

In this study, aerial robots' autonomous motions were improved by the intelligent method of fuzzy logic. The graph theory considering information linkages between aerial robots was used to enhance the accuracy of the proposed guidance. Each aerial robot contains information received from others to determine the positions. Linkages are denoted by $\alpha\vec{\ell}$, where α is a design coefficient $\alpha \in [0, 1]$, and $\vec{\ell}$ is a vector possessing information of aerial robots. $\vec{\ell}$ is a function of position \vec{R} ,

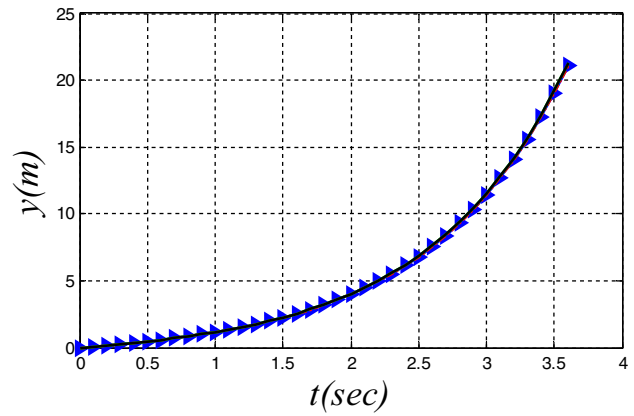


Fig. 15 Time history of y(t) regarding damping uncertainties of the control variable

where $\vec{R} = [x, y, z]$. The quality of information is shown by $\vec{\Omega}$, and the distance from the destination is denoted by $\vec{\mathfrak{S}}$. Therefore, information linkages can be denoted as $\ell = \ell(\vec{R}, \vec{\Omega}, \vec{\mathfrak{S}})$.

It should be noted that $\vec{\Omega}$ can be a function of the received information from GPS and distance to the destination $\vec{\mathfrak{S}}$ implicitly. There are many $\vec{\ell}$ linkages between aerial robots. Based on ℓ_{sr} between aerial robot (s) and aerial robot (r), the fuzzy rules are constructed to guide the aerial robots intelligently by increasing the proposed guidance quality. Hence, ℓ_{sr} can be formulated as below:

$$\ell_{sr}^P = \left| \overline{\zeta}(s) - \overline{\zeta}(s+1) \right|_{r=s+1} \tag{25}$$

where $\overline{\zeta}(\cdot)$ is the vector of the position for aerial robots. Index (s) and (s+1) are considered because the aerial robot (s) and (s+1) are closed to each other, thereby transferring information better. Furthermore, ℓ'_{sr} is considered as:

$$\ell'_{sr}{}^P = \left| \overline{\zeta}(s) - \overline{\zeta}(e) \right|_{e=random} \tag{26}$$

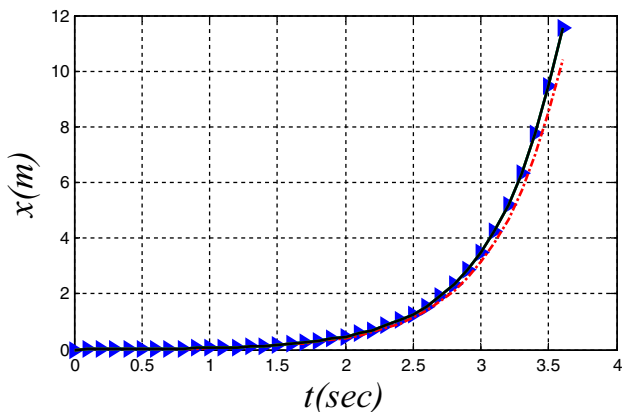


Fig. 14 Time history of x(t) regarding damping uncertainties of the control variable

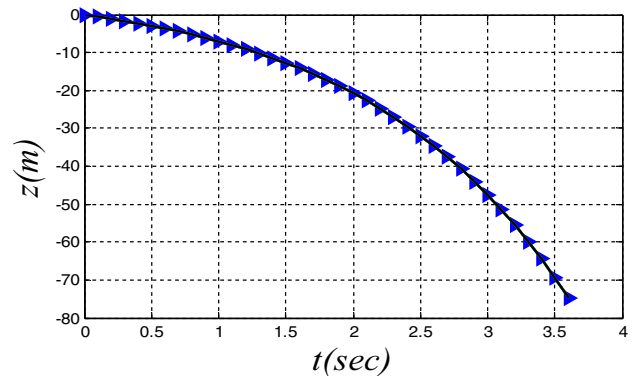


Fig. 16 Time history of z(t) regarding damping uncertainties of the control variable

The information linkage between aerial robot (s) and other aerial robots is considered as random aerial robots' position. Accordingly, all the transform linkages can be evaluated. The linkages include two vectors and one constant as $\vec{\ell}_{sr} = \ell_{sr}(\vec{R}, \vec{\Omega}, \mathfrak{F})$ and $\vec{\ell}'_{sr} = \ell'_{sr}(\vec{R}, \vec{\Omega}, \mathfrak{F})$. Some information about the positions of aerial robots is achieved from GPS, and the positions' vectors are also obtained.

The main problem here is how to use ℓ_{sr} or ℓ'_{sr} in the proposed guidance. The answer is to exploit the fuzzy logic. Based on the defined fuzzy rules, the aerial robots' decisions are made to increase the operation for converging more qualified results. The mentioned fuzzy logic method is considered for A-type aerial robots. Therefore, aerial robots' swarm guidance is developed based on data received from GPS and fuzzy logic decisions. Some rules for fuzzy logic are illustrated below:

1. If there is not GPS signal then high usual behavior of algorithm is considered.
2. If GPS signal is low then high usual behavior of algorithm is considered.
3. If GPS signal is high then low usual behavior of algorithm is considered.
4. If there is not ℓ_{sr} or ℓ'_{sr} signal then usual behavior of algorithm is considered.
5. If ℓ_{sr} or ℓ'_{sr} signal is high then low usual behavior of algorithm is considered.
6. If ℓ_{sr} is high and ℓ'_{sr} is low then medium behavior of algorithm is considered.
7. If ℓ_{sr} is high and ℓ'_{sr} is high then low behavior of algorithm is considered.
8. If ℓ_{sr} is low and ℓ'_{sr} is low then high behavior of algorithm is considered.

Five bell-shaped membership functions are considered for the fuzzification and defuzzification of the fuzzy logic. Moreover, the weights of rules are equal to 1, and the Mamdani method is considered for the inference system.

The nature-inspired guidance illustrated in this study is improved by the fuzzy logic; hence, the proposed fuzzy

logic-integrated nature-inspired guidance provides more precise results. Table 2 presents the comparison of two proposed guidance methods of fuzzy logic-integrated nature-inspired guidance and nature-inspired guidance algorithms, indicating the former's high accuracy.

According to Table 2, the fuzzy logic-integrated nature-inspired guidance has a lower total passing (decreasing 24.64%) and final time (decreasing 21.87%) for aerial robots.

In order to better study the fuzzy logic, 20 aerial robots are considered in Fig. 17. Figure 17 demonstrates the location of 20 aerial robots without considering fuzzy logic. In this way, Fig. 18 shows the communication links of aerial robots at the beginning of the use of fuzzy logic. After using fuzzy logic and improving the communication network between the aerial robots, their convergence increases. For

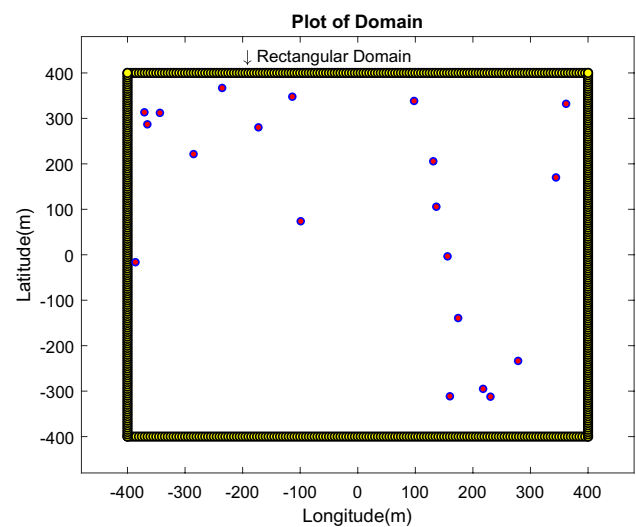


Fig. 17 Aerial robots' distribution

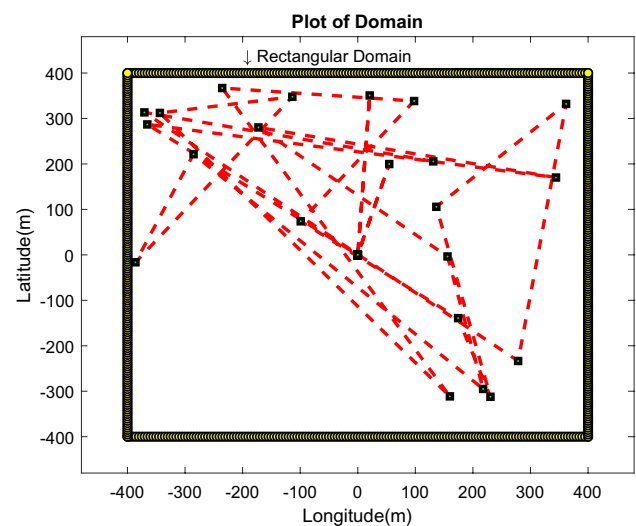


Fig. 18 Fuzzy linkages for aerial robots

Table 2 Comparison two proposed guidance

	Nature-inspired guidance	Integrated nature-inspired guidance by fuzzy logic
The total path for all aerial robots (50 aerial robots)	8536 (m)	6432 (m)
Final time for all aerial robots (50 aerial robots)	32 (s)	25 (s)

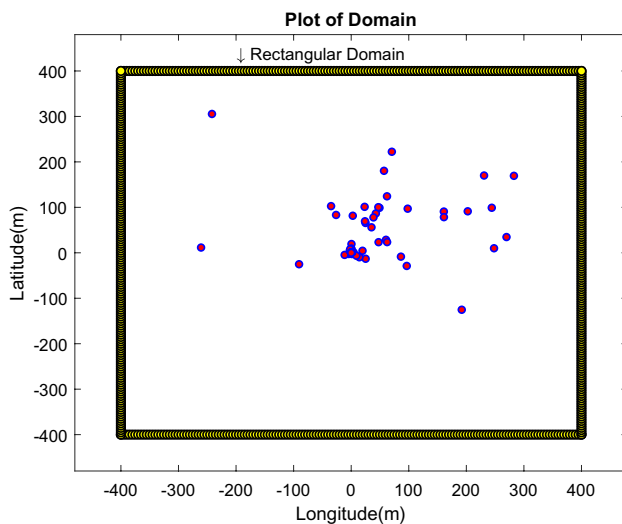


Fig. 19 Converging of aerial robots regarding enhancing by fuzzy logic

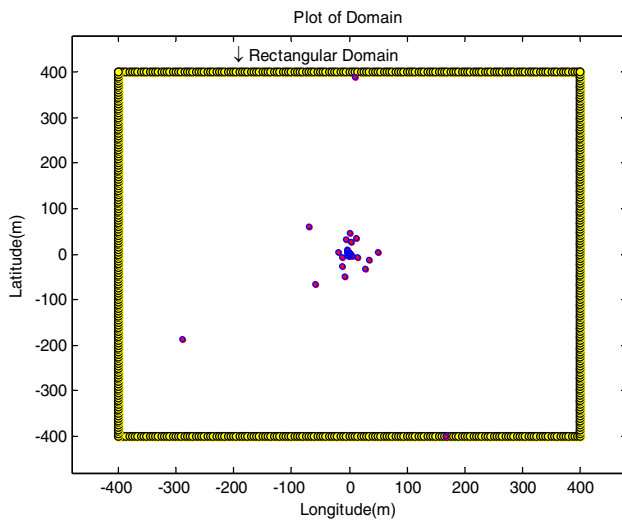


Fig. 20 Final convergence of aerial robots regarding enhancing by fuzzy logic

a better review of the upgrade of the mentioned intelligent guidance, Fig. 19 is given. By comparing Figs. 17 and 18, the behaviors of the improved aerial robots by fuzzy logic are emphasized. Finally, Fig. 20 shows the convergence of aerial robots based on fuzzy logic.

8 Conclusion

This study focused on a nature-inspired autonomous algorithm for multiple aerial robots. This algorithm was considered not only as a novel nature-based autonomous guidance but also as an autonomous method. Considering a decrease

in flight mechanics' calculations, a new equation system was proposed based on the derivatives by the yaw control angle. Moreover, the neural-fuzzy network as one of the powerful methods was applied to decrease different uncertainties such as lateral wind current and navigation' noise. The neural-fuzzy network was proved to be highly efficient in estimating, approximating, and increasing reliability. To implement the intelligent neural-fuzzy system, several flight scenarios are selected. Accordingly, three flight scenarios were selected with close boundary conditions here. The yaw control angle accomplished the dynamic system training by artificial intelligence as the neural-fuzzy network output. The proposed neural-fuzzy network could deliver the aerial robots by high reliability and consider uncertainties from the initial point to the path's endpoint. According to the results, aerial robots' precision in arriving at the target increased from 31.62 to 67.32% for different lateral wind currents and navigation' noise. Moreover, aerial robots' autonomous motions were improved by the fuzzy logic to develop information linkages between aerial robots with a lower total passing and final times of 24.64% and 21.87%, respectively. In sum, autonomous aerial robots could be designed intelligently using a novel combination of the bee algorithm, neural-fuzzy network, and fuzzy logic.

References

- Al-Rabayah M, Malaney R (2012) A new scalable hybrid routing protocol for VANETs. *IEEE Trans Veh Technol* 61:2625–2635
- Babaei AR, Mortazavi M, Moradi MH (2011) Classical and fuzzy-genetic autopilot design for unmanned aerial vehicles. *Appl Soft Comput* 11:365–372
- Bernsen J, Manivannan D (2012) RIVER: a reliable inter-vehicular routing protocol for vehicular ad hoc networks. *Comput Netw* 56:3795–3807
- Bitam S, Mellouk A, Zeadally S (2013) HyBR: a hybrid bio-inspired bee swarm routing protocol for safety applications in vehicular ad hoc networks (VANETs). *J Syst Archit* 59:953–967
- Chen Y, Yu J, Mei Y et al (2016) Modified central force optimization (MCFO) algorithm for 3D UAV path planning. *Neurocomputing* 171:878–888
- Chen Y, Jia Z, Ai X et al (2017) A modified two-part wolf pack search algorithm for the multiple traveling salesmen problem. *Appl Soft Comput* 61:714–725
- Dadkhah N, Mettler B (2012) Survey of motion planning literature in the presence of uncertainty: considerations for UAV guidance. *J Intell Robot Syst* 65:233–246
- Eng P, Mejias L, Liu X, Walker R (2010) Automating human thought processes for a UAV forced landing. *J Intell Robot Syst* 57:329
- Fallah-Zazuli M, Vafaeinejad A, Alesheykh AA et al (2019) Mapping landslide susceptibility in the Zagros Mountains, Iran: a comparative study of different data mining models. *Earth Sci Inform* 12:615–628
- Goerzen C, Kong Z, Mettler B (2010) A survey of motion planning algorithms from the perspective of autonomous UAV guidance. *J Intell Robot Syst* 57:65

- Hoffer NV, Coopmans C, Jensen AM, Chen Y (2014) A survey and categorization of small low-cost unmanned aerial vehicle system identification. *J Intell Robot Syst* 74:129–145
- Huang L, Qu H, Ji P et al (2016) A novel coordinated path planning method using k-degree smoothing for multi-UAVs. *Appl Soft Comput* 48:182–192
- Lange S, Sunderhauf N, Protzel P (2009) A vision based onboard approach for landing and position control of an autonomous multirotor UAV in GPS-denied environments. In: 2009 International conference on advanced robotics, IEEE, pp 1–6
- Laomettachit T, Termsaithong T, Sae-Tang A, Duangphakdee O (2015) Decision-making in honeybee swarms based on quality and distance information of candidate nest sites. *J Theor Biol* 364:21–30
- Liu Y, Zhang X, Guan X, Delahaye D (2016) Adaptive sensitivity decision based path planning algorithm for unmanned aerial vehicle with improved particle swarm optimization. *Aerosp Sci Technol* 58:92–102
- Luo Q, Yang X, Zhou Y (2019) Nature-inspired approach: an enhanced moth swarm algorithm for global optimization. *Math Comput Simul* 159:57–92
- Ma L, Stepanyan V, Cao C et al (2006) Flight test bed for visual tracking of small UAVs. In: AIAA guidance, navigation, and control conference and exhibit, p 6609
- Mavrovouniotis M, Li C, Yang S (2017) A survey of swarm intelligence for dynamic optimization: algorithms and applications. *Swarm Evol Comput* 33:1–17
- Mettler B, Dadkhah N, Kong Z (2010) Agile autonomous guidance using spatial value functions. *Control Eng Pract* 18:773–788
- Moayedi H, Hayati S (2018a) Modelling and optimization of ultimate bearing capacity of strip footing near a slope by soft computing methods. *Appl Soft Comput* 66:208–219
- Moayedi H, Hayati S (2018b) Applicability of a CPT-based neural network solution in predicting load-settlement responses of bored pile. *Int J Geomech* 18:6018009
- Moayedi H, Rezaei A (2019) An artificial neural network approach for under-reamed piles subjected to uplift forces in dry sand. *Neural Comput Appl* 31:327–336
- Moayedi H, Tien Bui D, Gör M et al (2019) The feasibility of three prediction techniques of the artificial neural network, adaptive neuro-fuzzy inference system, and hybrid particle swarm optimization for assessing the safety factor of cohesive slopes. *ISPRS Int J Geo Inf* 8:391
- Moayedi H, Moatamediyan A, Nguyen H et al (2020) Prediction of ultimate bearing capacity through various novel evolutionary and neural network models. *Eng Comput* 36:671–687
- Mosallanezhad M, Moayedi H (2017) Developing hybrid artificial neural network model for predicting uplift resistance of screw piles. *Arab J Geosci* 10:479
- Nguyen H, Mehrabi M, Kalantar B et al (2019) Potential of hybrid evolutionary approaches for assessment of geo-hazard landslide susceptibility mapping. *Geomat Nat Hazards Risk* 10:1667–1693
- Paw YC, Balas GJ (2011) Development and application of an integrated framework for small UAV flight control development. *Mechatronics* 21:789–802
- Rajasekhar A, Lynn N, Das S, Suganthan PN (2017) Computing with the collective intelligence of honey bees—a survey. *Swarm Evol Comput* 32:25–48
- Samani M, Tafreshi M, Shafieenejad I, Nikkhah AA (2015) Minimum-time open-loop and closed-loop optimal guidance with GA-PSO and neural fuzzy for Samarai MAV flight. *IEEE Aerosp Electron Syst Mag* 30:28–37
- Torres M, Pelta DA, Verdegay JL, Torres JC (2016) Coverage path planning with unmanned aerial vehicles for 3D terrain reconstruction. *Expert Syst Appl* 55:441–451
- Zedadra O, Guerrieri A, Jouandeau N et al (2018) Swarm intelligence-based algorithms within IoT-based systems: a review. *J Parallel Distrib Comput* 122:173–187
- Zhou Y, van Kampen E-J, Chu Q (2019) Hybrid hierarchical reinforcement learning for online guidance and navigation with partial observability. *Neurocomputing* 331:443–457
- Zhou G, Moayedi H, Bahiraei M, Lyu Z (2020) Employing artificial bee colony and particle swarm techniques for optimizing a neural network in prediction of heating and cooling loads of residential buildings. *J Clean Prod* 254:120082

Publisher's Note Springer Nature remains neutral with regard to jurisdictional claims in published maps and institutional affiliations.